Supporting Information

Design and Engineering of Novel Extrusion-Cast Films from Plasticized Cellulose Acetate Filled with Mineral Fillers for Flexible Packaging Applications

Fatemeh Jahangiri[1,2], Matias Menossi[1,2], Manjusri Misra[1,2] and Amar K. Mohanty,[1,2*]*

[1]Bioproducts Discovery and Development Centre, Department of Plant Agriculture, Crop Science Building, University of Guelph, 50 Stone Road East, Guelph, Ontario, Canada.

[2]Department of Interdisciplinary Engineering, College of Engineering, THRN Building, University of Guelph, Guelph, Ontario, N1G 2W1, Canada.

Corresponding Authors:

*Manjusri Misra; Email: mmisra@uoguelph.ca; ORCID: 0000-0003-2179-7699

*Amar K. Mohanty; Email: mohanty@uoguelph.ca; ORCID: 0000-0002-1079-2481

Degree of substitution (DS) and Molecular weight (MW) of the cellulose acetate

The degree of substation (DS) of the cellulose acetate (CA) was calculated based on **Equation S1** [1]. The %acetyl content in **Equation S1** was calculated based on **Equation S2** [1]. The combined acetic acid content was provided in the CA's technical datasheet (TDS) which is equal to 52.8%. Therefore, the calculated DS for the CA used in this study was 2.26. One of the main benefits of CA is its biodegradability, making it a promising material for sustainable and eco-friendly packaging. The rate at which CA biodegrades is influenced by its DS, which generally ranges from 1.7 to 3.0. A lower DS increases biodegradability because the polymer contains more hydroxyl (-OH) groups and fewer acetyl groups in its structure [2]. Hence, in this study, CA with a low DS (i.e., 2.26) was selected.

$$DS = \frac{3.86 \times \%\, acetyl}{102.4 - \%\, acetyl} \qquad \text{(S1)}$$

$$Combined\ acetic\ acid = acetyl\ content \times 1.395 \qquad \text{(S2)}$$

The molecular weight of the CA was calculated based on **Equation S3**, where *DP* is the degree of polymerization (i.e., 185 for the CA used in this study based on its TDS) and M_n is the number average molecular weight of polymer and *m* is the molecular weight of the repeat unit. The *m* was calculated based

on the CA's chemical structure, which is equal to 492.425 g/mol. Therefore, the calculated number average molecular weight for the CA used in this study was 91098.721 g/mol.

$$\bar{M}_n = DP \times m \qquad \text{(S3)}$$

Rheological Properties

Rheological characteristics are important for understanding the behavior of a molten polymer under shear forces. Particularly, to understand the interactions at the macromolecular level, including polymeric chain architecture, phase morphology as well as type of reaction (cross-linking, scissions, grafting), etc [3]. The complex viscosity versus angular frequency (**Figure S1 a-d**) as well as storage and loss modulus (**Figure S2 a-d**) performed on neat pCA pellets as well as pCTEC/0.01LUP and pCTA/0.01LUP, and their composites.

All samples exhibited a non-Newtonian shear thinning behavior; as the shear rate increased, the complex viscosity decreased gradually. This phenomenon is attributed to the interactions between polymeric molecules and plasticizer and fillers, which can result in reduction of CA chain interactions and disentanglement at higher shear rates [4]. When organic peroxide was introduced into pCTA or pCTEC the complex viscosity increased across all angular frequencies **(Figure S1 a, c)**. Menossi et al. [3] and Ma et al. [5] observed the same trend after addition of peroxide compound to PBAT/pCA blends and PBAT/PLA blends, respectively, which was associated with crosslinked structures. Addition of 10% talc or $rCaCO_3$ resulted in an increase in complex viscosity for pCTEC/10Talc, pCTEC/10$rCaCO_3$, pCTA/10Talc, pCTA/10$rCaCO_3$ compared to their corresponding neat pCTEC or pCTA samples. This increase in complex viscosity is due to restriction of polymeric chains mobility induced by the filler loading. Similar behaviour were observed in the previous literature by addition of microcrystalline cellulose to pCA matrix [6].

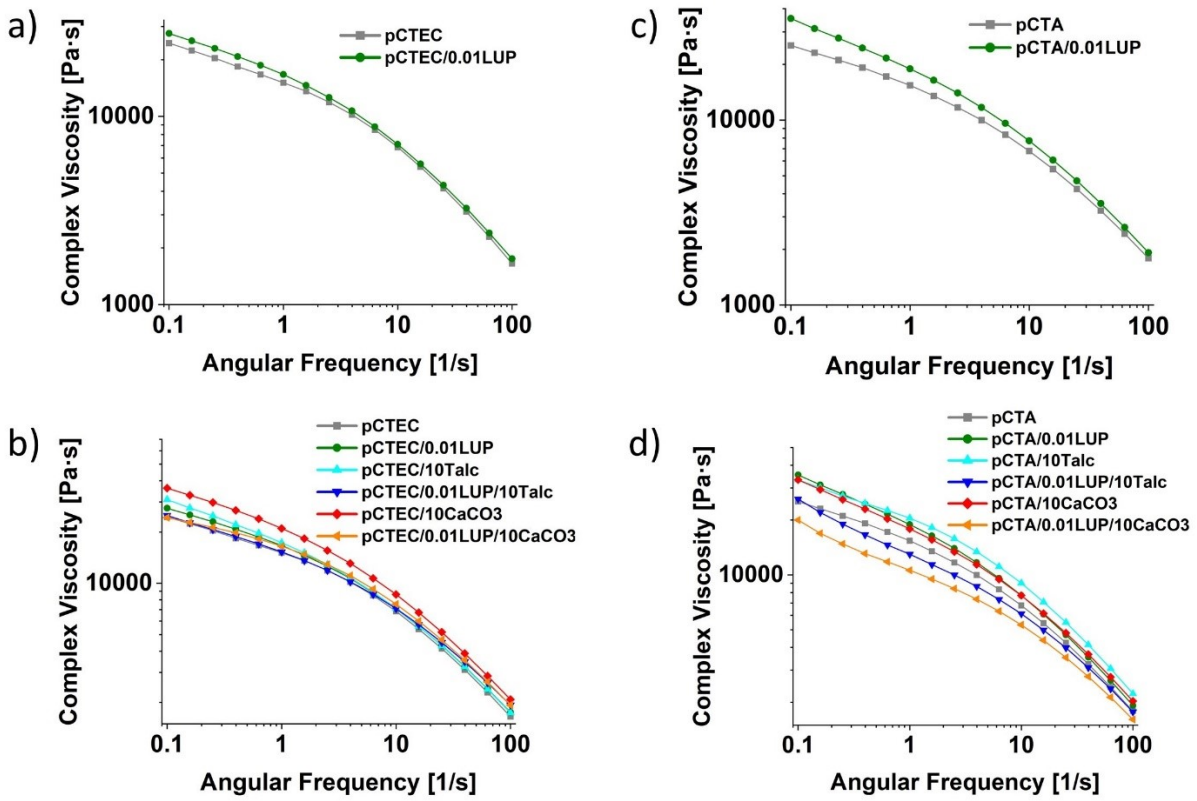

Figure S1: Complex viscosity versus angular frequency; a) pCTEC and pCTEC/0.01LUP, b) pCTEC-based composites, c) pCTA and pCTA/0.01LUP, d) pCTA-based composites. pCTEC: plasticized cellulose acetate with triethyl citrate, pCTA: plasticized cellulose acetate with triacetin, TEC: triethyl citrate, TA: triacetin, LUP: luperox, $rCaCO_3$: recycled calcium carbonate

The incorporation of both fillers (either talc or $rCaCO_3$) within LUP into pCA (either plasticized with TA or TEC), however, resulted in a reduction in complex viscosity compared to only pCA-filled filler (**Figure S1 b,d**). This is due to presence of LUP that improved filler dispersion, thereby reducing agglomeration which resulted in lower complex viscosity. In our previous study, we showed that in presence of LUP, talc shows easier delamination and better interaction with pCA matrix [7]. This improved filler dispersion can reduce microstructural viscosity buildup. The LUP acted as a compatibilizer between pCA matrix and the filler, which can result in better filler dispersion and reduction of filler-filler contact, thereby reducing complex viscosity. This is the same mechanism often observed in compatibilized polymer composites. For example, Garcia Castellanos et al. [6] reported a decrease after addition of maleic anhydride-grafted-cellulose acetate into pCA/microcryslline cellulose composites. The reduction in complex viscosity can be due to low molecular weight compatibilizer acting as a plasticizing agents in the matrix [6, 8]. The incorporation of nanosilica (0–0.7 vol%) into polycarbonate with a molecular weight of 31.5 kg/mol has

been shown to reduce the complex viscosity relative to the neat polymer. This reduction is attributed to a lower entanglement density surrounding the nanoparticles and to the long relaxation times of these networks at low frequencies, which predominantly influence the rheology of the nanocomposites [9]. Similarly, another study reported that polystyrene nanocomposites containing silica or graphene displayed reduced complex viscosity compared with the pure polymer, and that the viscosity became stable and insensitive to further increases in filler content [10].

The storage and loss moduli in **Figure S2 (a-d)** showed a similar trend to that observed in complex viscosity. With increasing angular frequency, the modulus of all samples increased, indicating that neat pCA (either plasticized with TA or TEC), as well as their composites follow the theory of linear viscoelasticity [11]. The storage modulus reflects how elastically a polymer or polymer composite responds, indicating the amount of energy it can retain when it is deformed. In contrast, the loss modulus highlights the material's viscous characteristics, describing how it dissipates energy during deformation. Similar to complex viscosity trends, the incorporation of both fillers (either talc or $rCaCO_3$) within LUP into pCA samples, resulted in a reduction in storage and loss modulus. Similarly, addition of a compatibilizer into pCA/microcrystalline cellulose resulted in a reduction in storage and loss modulus of pCA matrix [6].

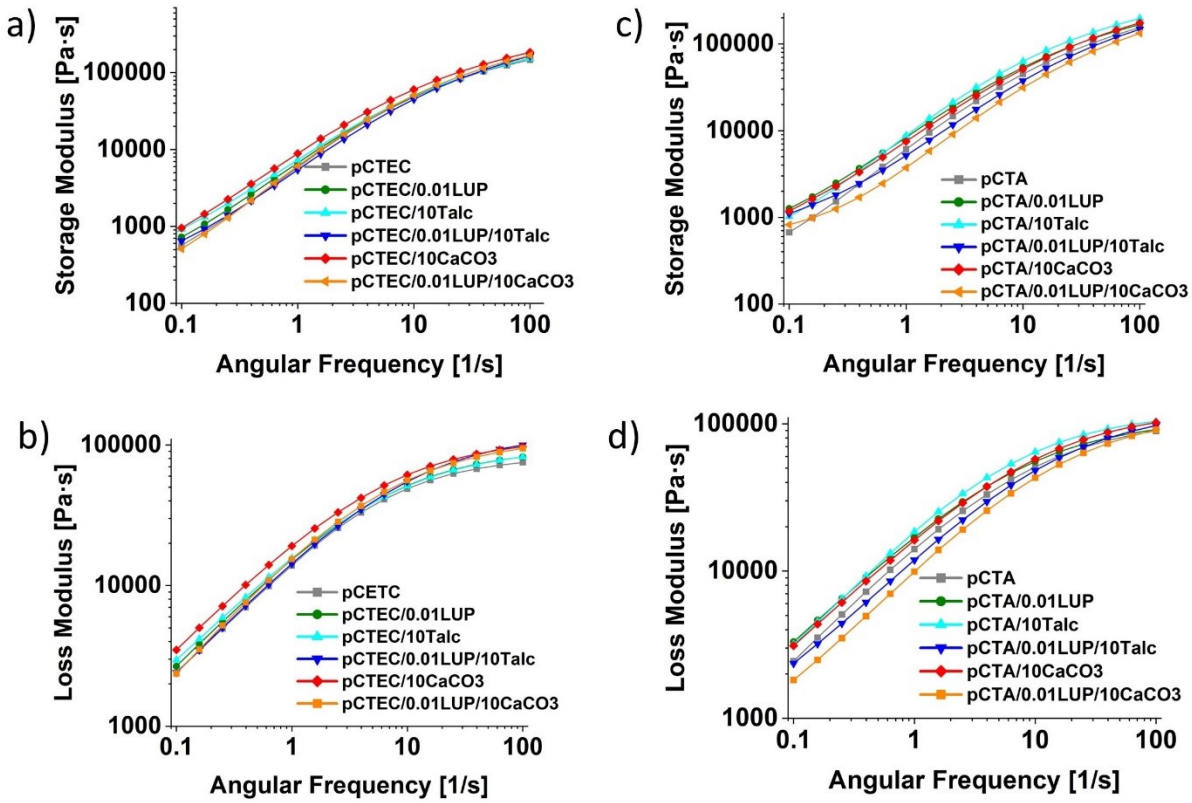

Figure S2: Rheological properties; a) storage modulus of pCTEC and pCTEC-based composites, b) loss

modulus of pCTEC and pCTEC-based composites, c) storage modulus of pCTA and pCTA-based composites, d) loss modulus of pCTA and pCTA-based composites. pCTEC: plasticized cellulose acetate with triethyl citrate, pCTA: plasticized cellulose acetate with triacetin, TEC: triethyl citrate, TA: triacetin, LUP: luperox, $rCaCO_3$: recycled calcium carbonate

Water Vapor Absorption (WVA)

The equilibrium water vapor absorption (WVA_{eq}), defined as the maximum WVA reached in each sorption curve, is summarized in **Table S1**. Clear differences were observed between the pCTA and pCTEC formulations at 60 and 90% of relative humidity (RH) levels evaluated. Incorporation of TEC as a plasticizer into the cellulose acetate (CA) matrix significantly increased WVA_{eq} under both humidity conditions, with values approximately twice those measured for the TA-plasticized samples. As expected, higher RH led to greater WVA_{eq} values [12, 13].

These findings are consistent with the SEM observations, water contact angle measurements, and barrier performance results discussed in **Sections 3.3**, **3.4** and **3.5,** respectively. The behavior can be attributed to differences in chemical structure: TEC contains an additional hydroxyl (–OH) group, which enhances its affinity for water vapor and promotes stronger polymer–water interactions, thereby increasing moisture uptake.

Table S1: The equilibrium water vapor absorption values of neat pCA films. pCTEC: plasticized cellulose acetate with triethyl citrate, pCTA: plasticized cellulose acetate with triacetin, TEC: triethyl citrate, TA: triacetin.

Sample	WVA_{eq} (%) 60% RH	WVA_{eq} (%) 90% RH
pCTA	0.74 (0.29)	2.82 (0.50)
pCTEC	1.49 (0.16)	4.46 (0.40)

Scanning Electron Microscopy (SEM)

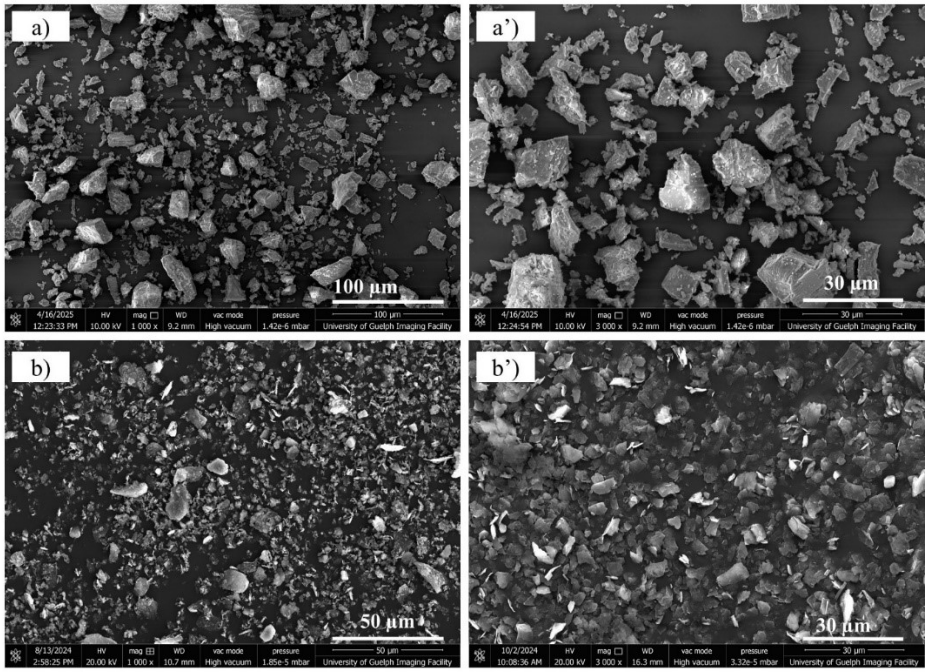

Figure S3: The SEM images of a, a') $rCaCO_3$ and b, b') Talc powder at 1000× and 3000× magnifications. [$rCaCO_3$: recycled calcium carbonate]

Water contact angle and surface energy

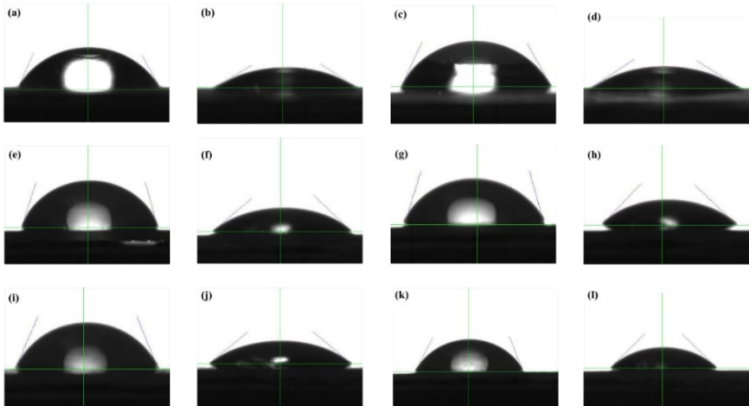

Figure S4. Water contact angle of neat biodegradable polymers, a) pCTA, c) pCTA/0.01LUP, e) pCTA/0.01LUP/10 Talc, g) pCTA/0.01LUP/15 Talc, i) pCTA/0.01LUP/10 $rCaCO_3$, k) pCTA/0.01LUP/15 $rCaCO_3$. Diiodomethane contact angle of, b) pCTA, d) pCTA/0.01LUP, f) pCTA/0.01LUP/10 Talc, h) pCTA/0.01LUP/15 Talc, j) pCTA/0.01LUP/10 $rCaCO_3$, l) pCTA/0.01LUP/15 $rCaCO_3$. pCTEC: plasticized cellulose acetate with triethyl citrate, pCTA: plasticized cellulose acetate with triacetin, TEC: triethyl citrate, TA: triacetin, LUP: luperox, $rCaCO_3$: recycled calcium carbonate

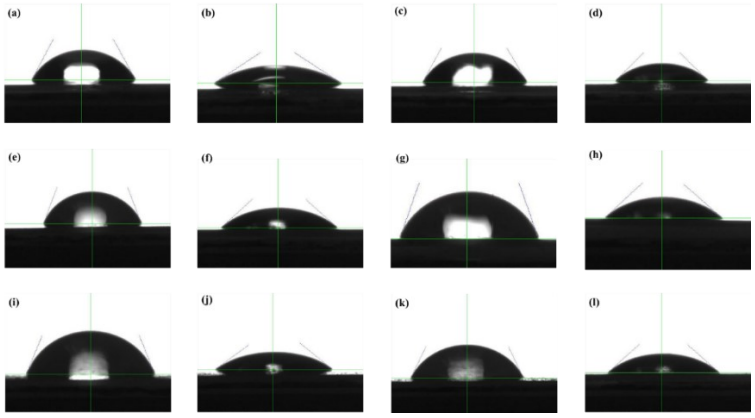

Figure S5. Water contact angle of neat biodegradable polymers, a) pCTEC, c) pCTEC/0.01Lup, e) pCTEC/0.01LUP/10 Talc, g) pCTEC/0.01LUP/15 Talc, i) pCTEC/0.01LUP/10 $rCaCO_3$, k) pCTEC/0.01LUP/15 $rCaCO_3$. Diiodomethane contact angle of, b) pCTEC, d) pCTEC/0.01Lup, f) pCTEC/0.01LUP/10 Talc, h) pCTEC/0.01LUP/15 Talc, j) pCTEC/0.01LUP/10 $rCaCO_3$, l) pCTEC/0.01LUP/15 $rCaCO_3$. pCTEC: plasticized cellulose acetate with triethyl citrate, pCTA: plasticized cellulose acetate with triacetin, TEC: triethyl citrate, TA: triacetin, LUP: luperox, $rCaCO_3$: recycled calcium carbonate

Oxygen permeation (OP) and Water vapor permeation (WVP)

Table S2: The water vapor and oxygen permeation values of neat pCA films and pCA-based composite films. pCTEC: plasticized cellulose acetate with triethyl citrate, pCTA: plasticized cellulose acetate with triacetin, TEC: triethyl citrate, TA: triacetin, LUP: luperox, $rCaCO_3$: recycled calcium carbonate

Sample	**WVP (gm.mil/m².day)**	**OP (cc.mil/m².day)**
pCTA	1598.86 (84.14)	1986.93 (102.31)
pCTA/0.01Lup	1958.78 (10.19)	2617.72 (99.33)
pCTA/0.01LUP/10Talc	1144.38 (17.84)	1565.76 (41.06)
pCTA/0.01LUP/15Talc	1098.42 (27.17)	1303.95 (150.54)
pCTA/0.01LUP/10$rCaCO_3$	1758.31 (74.58)	1716.64 (325.95)
pCTA/0.01LUP/15$rCaCO_3$	1629 (11.84)	1768.01 (21.21)
pCTEC	3267.60 (38.94)	2462.99 (54.391)
pCTEC/0.01Lup	2664.45 (82.22)	2367.33 (40.87)
pCTEC/0.01LUP/10Talc	1163.19 (33.12)	1817.79 (56.62)
pCTEC/0.01LUP/15Talc	913.18 (2.40)	1520.17 (13.88)
pCTEC/0.01LUP/10$rCaCO_3$	1446.93 (25.81)	2417.36 (83.39)
pCTEC/0.01LUP/15$rCaCO_3$	1398.17 (135.47)	2401.74 (42.39)

Fourier Transformed Infrared Spectroscopy

The FTIR analysis was carried out on talc and $rCaCO_3$ powder as well as pCTA and pCTEC-based composite formulations to investigate the functional groups as well as chemical interactions between composite's components. The pCTA and pCTEC filled with talc or $rCaCO_3$ composite samples showed similar peaks in the FTIR as it is shown in **Figure S6**.

Recycled calcium carbonate, with the chemical formula of $CaCO_3$, showed the characteristic peaks with most intense bands of calcite at 715 cm^{-1} (ν_4, calcite), 870 cm^{-1} (ν_2, CO_3 out-of-plane bending) and 1400 cm^{-1}(ν_3, C-O stretching). The other bands can be corresponds to the capping agent, with lower intensity in comparison with those of carbonate ion [14]. Also, peaks observed at 1740 cm^{-1} (C=O), 2870 cm^{-1} and 2990 cm^{-1} (C-H) can be attributed to existence of organic compounds in $CaCO_3$ [14, 15] and peak at 3500 cm^{-1} corresponds to -OH groups of any absorbed water. Calcite is a natural polymorph of $CaCO_3$ [15]. The pCA-filled $CaCO_3$ showed the peak at 870 cm^{-1} which is enlarged in **Figure S6 (b,d)**. In addition, the peaks in the pCTA or pCTEC filled with $rCaCO_3$ composites at 1370-1500 $cm^{-1}$and 1740 cm^{-1} are impacted and showed lower intensities than pCTA/0.01LUP or pCTEC/0.01LUP due to the possible chemical interactions between filler and matrix. Similar observations were reported in the composites derived from high density polyethylene/oxidized polyethylene and $CaCO_3$ [16]. Other characteristic peaks of calcite overlapped with the pCTA or pCTEC characteristic peaks.

Talc is a hydrophobic additive composed of hydrated magnesium silicate, with the molecular formula $Mg_3Si_4O_{10}(OH)_2$. In its FTIR spectrum, prominent absorption bands are observed around 1000 cm^{-1}, with an accompanying shoulder near 1050 cm^{-1}, which are attributed to Si–O vibrations from the tetrahedral layer. Additional peaks appear at 670 cm^{-1} and approximately 3670 cm^{-1}, corresponding to vibrations associated with MgO/MgOH in the octahedral layer [17, 18].

For both pCTA and pCTEC, the FTIR spectra exhibit distinct bands at 2990 and 2870 cm^{-1} (linked to C–H stretching in $-CH_2$ and $-CH_3$ groups), 1740 cm^{-1} (C=O stretching in ester functionalities), 1370 cm^{-1} (bending vibrations of $-CH_3$ in acetyl groups), 1230 cm^{-1} (C–O stretching), and 1050 cm^{-1} (C–O–C stretching along the cellulose acetate backbone), as illustrated in **Figures S6 (a,c)**. This absorption features align with those previously reported for corresponding functional groups [6, 19]. A broad band centered at approximately 3500 cm^{-1} in the pCTEC and pCTA spectrum suggests the presence of residual unacetylated hydroxyl groups in the polymer structure.

The presence of peaks associated with both talc and cellulose acetate in the FTIR spectra of the composites demonstrates that the extrusion process preserved the chemical integrity of the materials without inducing detectable degradation. Moreover, incorporating 10 or 15 wt% talc into the pCTA/0.01LUP or pCTEC/0.01LUP matrix led to the emergence of peaks at ~1000 and 670 cm^{-1}, indicating successful integration of talc into the composites. Notably, addition of the talc amount (from 10 wt% to 15 wt%) enhanced the peak intensity at 670 cm^{-1}, as highlighted in the enlarged view in **Figures S6 (a,c)**. Similar

spectral patterns have also been observed in talc-reinforced composites such as PBAT and thermoplastic starch systems [20].

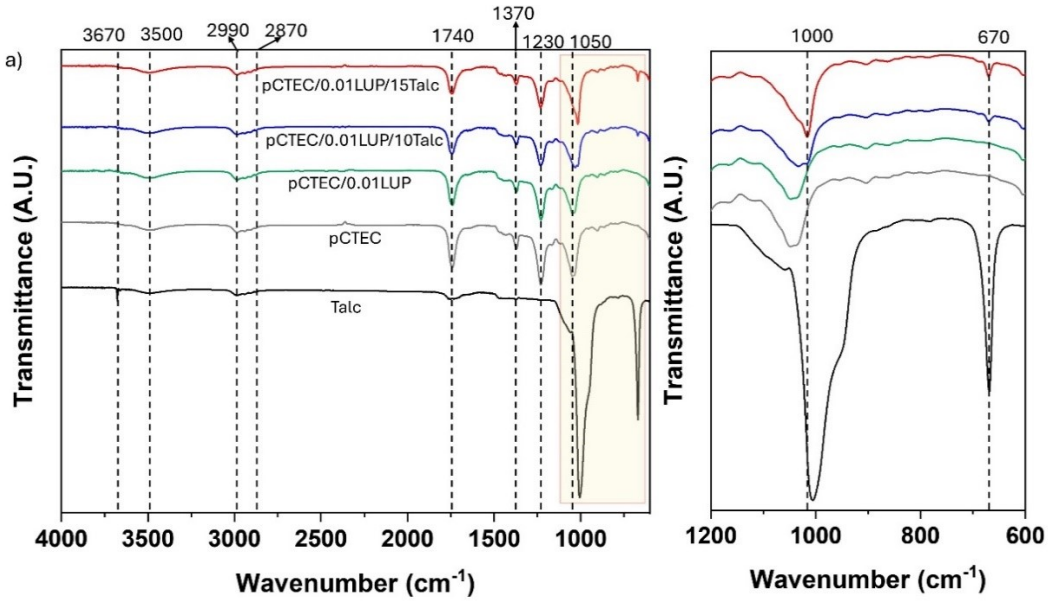
a)
3670
3500
2990
2870
1740
1370
1230
1050
1000
670
pCTEC/0.01LUP/15Talc
pCTEC/0.01LUP/10Talc
pCTEC/0.01LUP
pCTEC
Talc
Transmittance (A.U.)
Wavenumber (cm-1)
4000
3500
3000
2500
2000
1500
1000
1200
800
600

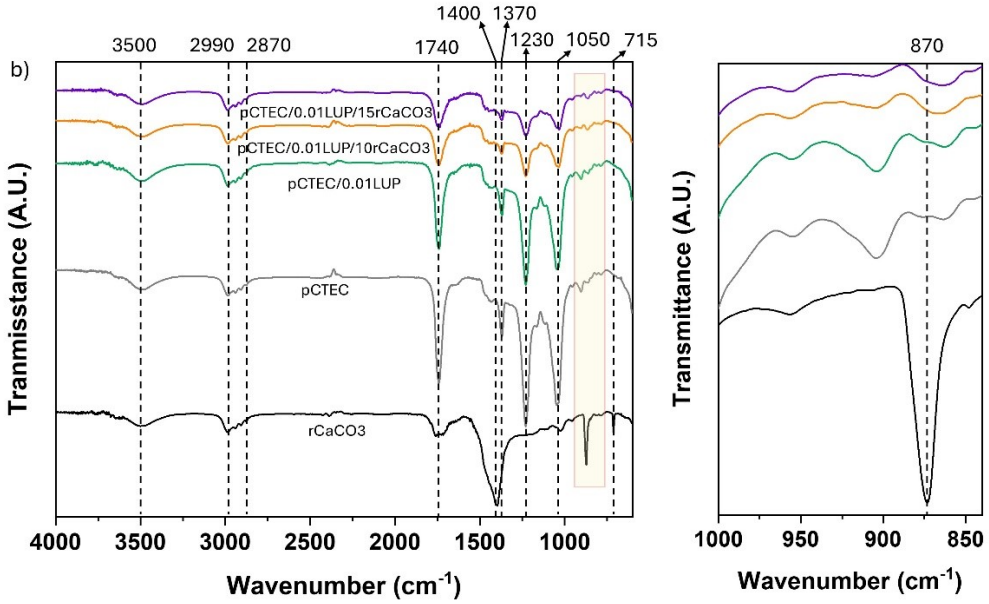
b)
3500
2990
2870
1740
1400
1370
1230
1050
715
870
pCTEC/0.01LUP/15rCaCO3
pCTEC/0.01LUP/10rCaCO3
pCTEC/0.01LUP
pCTEC
rCaCO3
Tranmisstance (A.U.)
Transmittance (A.U.)
Wavenumber (cm-1)
4000
3500
3000
2500
2000
1500
1000
950
900
850

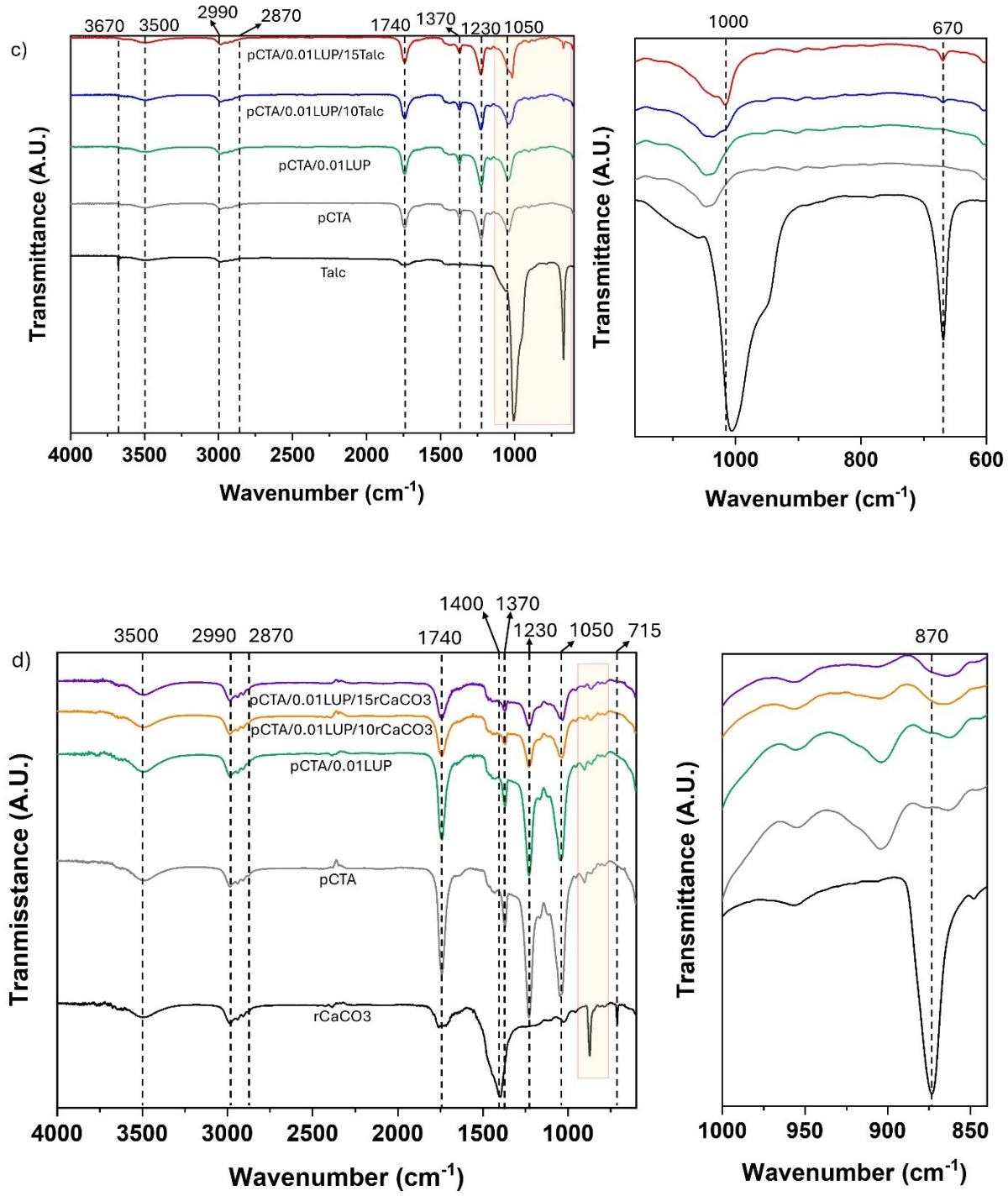

Figure S6: FTIR spectra of a) pCTEC filled talc composites, b) pCTEC filled $rCaCO_3$ composites, c) pCTA filled talc composites, d) pCTA filled $rCaCO_3$ composites. pCTEC: plasticized cellulose acetate with triethyl citrate, pCTA: plasticized cellulose acetate with triacetin, TEC: triethyl citrate, TA: triacetin, LUP: luperox, $rCaCO_3$: recycled calcium carbonate

Derivative Thermogravimetry (DTG)

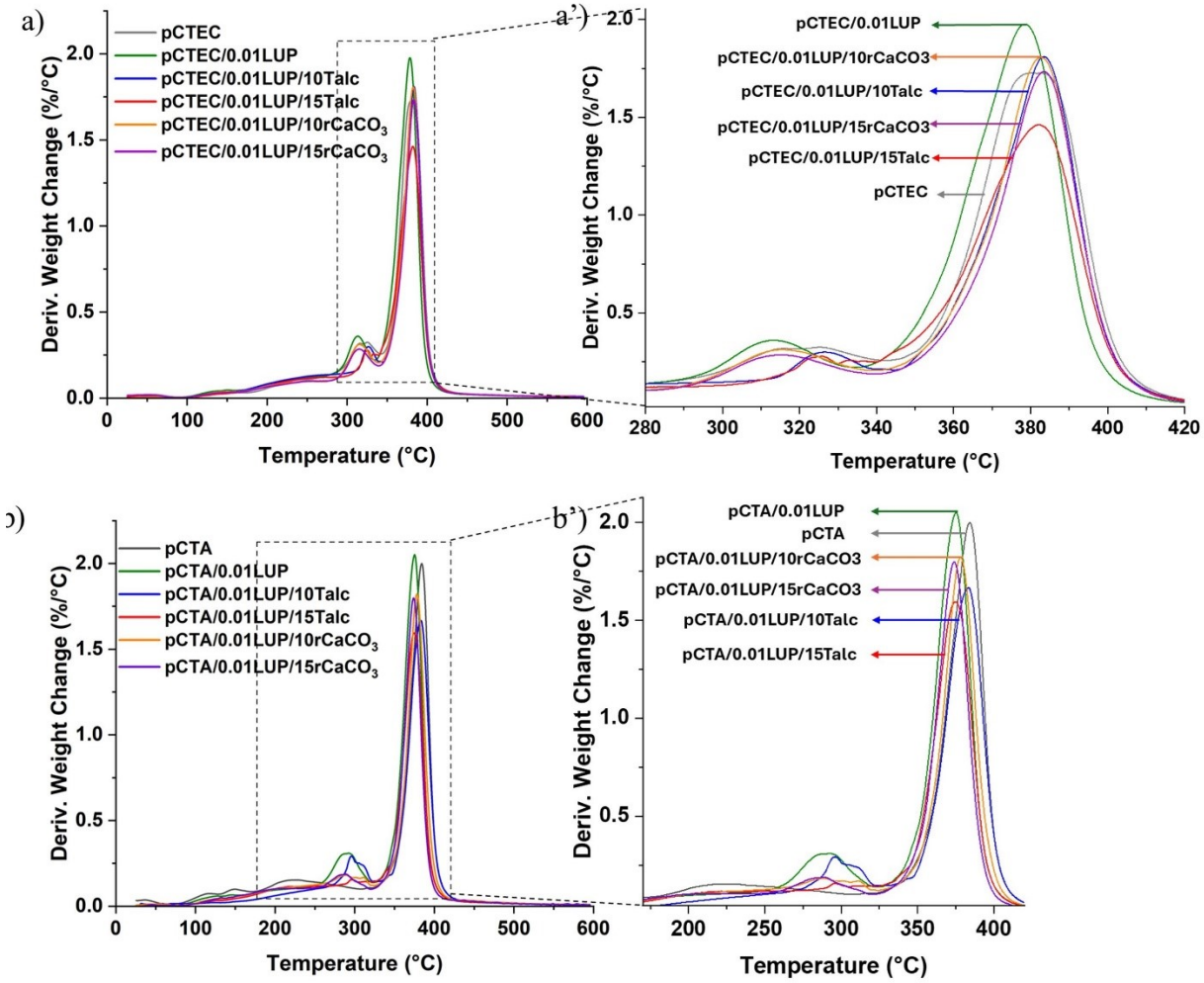

Figure S7: Derivative Thermograms of neat pCTA films and pCTEC films and composite films. a,a') pCTEC-based formulations. b,b') pCTA-based formulations. pCTEC: plasticized cellulose acetate with triethyl citrate, pCTA: plasticized cellulose acetate with triacetin, TEC: triethyl citrate, TA: triacetin, LUP: luperox, $rCaCO_3$: recycled calcium carbonate

References:

1. S. A. Ashter, *William Andrew Publishing*, 2018, 57-74.
2. V. T. Phuong, S. Verstiche, P. Cinelli, I. Anguillesi, M.-B. Coltelli and A. Lazzeri, *Journal of Renewable Materials*, 2014, **2**, 35-41.
3. M. Menossi, M. Misra and A. K. Mohanty, *ACS Applied Polymer Materials*, 2024, **6**, 10202-10217.
4. B. Wang, J. Chen, H. Peng, J. Gai, J. Kang and Y. Cao, *Journal of Macromolecular Science, Part B*, 2016, **55**, 894-907.
5. P. Ma, X. Cai, Y. Zhang, S. Wang, W. Dong, M. Chen and P. Lemstra, *Polymer Degradation and Stability*, 2014, **102**, 145-151.
6. I. García-Castellanos, D. Nath, R. Krishnan, M. Misra and A. K. Mohanty, *ACS Sustainable Resource Management*, 2025, **2(4)**, 594-604.
7. F. Jahangiri, M. Menossi, M. Misra and A. K. Mohanty, *Journal of applied polymer science*, 2025, e57973.
8. R. Muthuraj, M. Misra and A. K. Mohanty, *RSC advances*, 2017, **7**, 27538-27548.
9. V. Ramakrishnan, J. G. Goossens, T. L. Hoeks and G. W. Peters, *Nanomaterials*, 2021, **11**, 1839.
10. J. Zhu, C. Abeykoon and N. Karim, *International Journal of Lightweight Materials and Manufacture*, 2021, **4**, 370-382.
11. A. K. Pal, F. Wu, M. Misra and A. K. Mohanty, *Composites Part B: Engineering*, 2020, **198**, 108141.
12. F. Dubelley, E. Planes, C. Bas, E. Pons, B. Yrieix and L. Flandin, *The Journal of Physical Chemistry B*, 2017, **121**, 1953-1962.
13. H. M. Thijs, C. R. Becer, C. Guerrero-Sanchez, D. Fournier, R. Hoogenboom and U. S. Schubert, *Journal of Materials Chemistry*, 2007, **17**, 4864-4871.
14. C. Matei, D. Berger, A. Dumbrava, M. D. Radu and E. Gheorghe, *Journal of Sol-Gel Science and Technology*, 2020, **93**, 315-323.
15. J. Lv, J. Feng, W. Zhang, R. Shi, Y. Liu, Z. Wang and M. Zhao, *Journal of Forensic Sciences*, 2013, **58**, 134-137.
16. A. Ghosh, *Journal of Applied Polymer Science*, 2023, **140**, e53923.
17. O. Adi-Dako, F. W. A. Owusu, I. Y. Attah, D. Kumadoh, P. G. Acquah Jnr, I. Nelson, N. O. Hutton-Mills, K. Y. Y. Obese, J. A. Sarkodie and B. B. N'guessan, *Journal of Chemistry*, 2023, **1**, 8384739.
18. O. Adi-Dako, F. W. A. Owusu, I. Y. Attah, D. Kumadoh, P. G. Acquah Jnr, I. Nelson, N. O. Hutton-Mills, K. Y. Y. Obese, J. A. Sarkodie and B. B. N'guessan, *Journal of Chemistry*, 2023, **2023**, 8384739.
19. I. García-Castellanos, D. Nath, R. Krishnan, M. Misra and A. K. Mohanty, *ACS Sustainable Resource Management*, 2025.
20. A. Surendren, A. K. Pal, A. Rodriguez-Uribe, S. Shankar, L.-T. Lim, A. K. Mohanty and M. Misra, *International Journal of Biological Macromolecules*, 2023, **253**, 126751.